



ELSEVIER

Available online at www.sciencedirect.com

ScienceDirect

journal homepage: www.elsevier.com/locate/he

Cost-optimal design and energy management of fuel cell electric trucks

Alessandro Ferrara ^{a,*}, Stefan Jakubek ^a, Christoph Hametner ^b

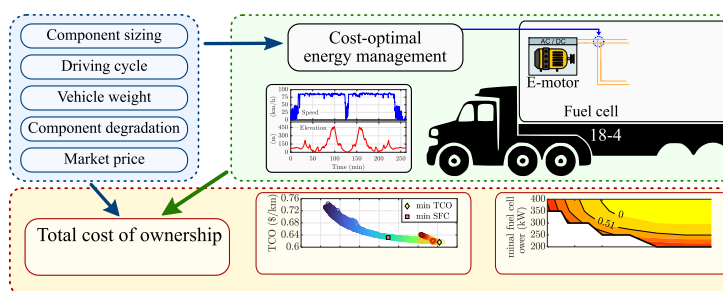
^a Institute of Mechanics and Mechatronics, Division of Process Control and Automation, TU Wien, 1060 Vienna, Austria

^b Christian Doppler Laboratory for Innovative Control and Monitoring of Automotive Powertrain Systems, TU Wien, 1060 Vienna, Austria

HIGHLIGHTS

- Investigation on total cost of ownership of heavy-duty fuel cell electric vehicles.
- Optimal vehicle design and control in demanding routes for performance requirements.
- Energy management optimization for minimum ownership cost in realistic driving scenarios.
- Trade-off analysis between fuel consumption and expected powertrain components life.
- Significant benefits of predictive energy management in challenging road topographies.

GRAPHICAL ABSTRACT



ARTICLE INFO

Article history:

Received 2 June 2022

Received in revised form

20 September 2022

Accepted 10 January 2023

Available online xxx

Keywords:

Energy management

Fuel cell vehicles

Optimal vehicle design

Total cost of ownership

ABSTRACT

Road freight transport on hilly routes represents a significant challenge for the advancement of fuel cell electric trucks because of the high-performance requirements for fuel consumption, vehicle lifetime, and battery charge control. Therefore, it is essential to optimize the vehicle design and energy management, which greatly influence the driving performance and total cost of ownership. This paper focuses on the cost-optimal design and energy management of fuel cell electric trucks, considering five key influencing factors: powertrain component sizing, driving cycle, vehicle weight, component degradation, and market prices. The cost optimization relies on a novel predictive energy management scheme based on dynamic programming and the systematic calibration of control parameters. The paper analyzes the simulation results to highlight three main findings for fuel cell electric trucks: 1) cost-optimal energy management is essential to define the best trade-off between fuel consumption and component degradation; 2) the total cost of ownership is significantly influenced by component sizing, driving cycles, vehicle weight,

* Corresponding author.

E-mail address: alessandro.ferrara@tuwien.ac.at (A. Ferrara).

<https://doi.org/10.1016/j.ijhydene.2023.01.110>

0360-3199/© 2023 The Author(s). Published by Elsevier Ltd on behalf of Hydrogen Energy Publications LLC. This is an open access article under the CC BY license (<http://creativecommons.org/licenses/by/4.0/>).

Powertrain component sizing
Dynamic programming

and market prices; 3) predictive energy management is highly beneficial in challenging road topographies for substantial cost-saving and lower component size requirements.

© 2023 The Author(s). Published by Elsevier Ltd on behalf of Hydrogen Energy Publications LLC. This is an open access article under the CC BY license (<http://creativecommons.org/licenses/by/4.0/>).

Introduction

The advancement and commercialization of fuel cell electric vehicles are hindered by high manufacturing and operating costs, limited battery and fuel cell life, and insufficient hydrogen fueling infrastructure. Moreover, road freight transport on hilly routes represents a significant challenge because of the high-performance requirements for fuel consumption, vehicle lifetime, and battery charge control. In recent years, increasing research effort has been focused on optimal powertrain design and control of hybrid electric vehicles to reduce their total cost of ownership (TCO), which is mainly influenced by the hydrogen operating cost and purchase costs of the powertrain components. Particular interest has been focused on energy management strategies due to their high impact on fuel consumption and component life. Indeed, this high-level control function performs the power-split between the fuel cell and battery systems, determining how the components are operated.

This paper studies the optimal design and energy management for minimum TCO, considering five key influencing factors: powertrain component sizing, driving cycle, vehicle weight, component degradation, and market prices (i.e. hydrogen, fuel cell, and battery costs). The investigation is focused on fuel cell electric trucks for road freight transport, which hold the highest potential for fuel cell automotive applications due to the high power and range requirements [1–3].

Literature survey

Energy management has been largely investigated in the last decade because of its high impact on vehicle performance. Indeed, energy management strategies (EMSs) have been designed using heuristic or optimal control methods for several hybrid electric vehicle configurations. A literature review on EMSs for engine-battery vehicles is proposed in Ref. [4], for fuel cell-battery vehicles in Refs. [5–7], and for fuel cell-ultracapacitor-battery vehicles in Ref. [8]. In general, one of the most studied methods for optimal energy management is dynamic programming (DP) because it allows finding the global optimum solution using the complete and a priori knowledge of the driving cycle [9]. Even though this method cannot be directly implemented for on-board control, DP has been widely used as a benchmark for the development of EMSs [10]. Even though the research interest in optimal energy management methods is generally stronger, a proper design of rule-based strategies can also be effective in terms of fuel consumption because the fuel cell system (FCS) efficiency characteristic is relatively flat in its average operating range [11]. However, ensuring high system efficiency and low component degradation is challenging for heavy-duty fuel cell

vehicles for freight transport on mountain roads. Health-conscious energy management strategies have been investigated considering component degradation within the optimization targets [12–16]. Recently, increasing research effort has been focused on predictive energy management strategies to find a good trade-off between fuel consumption, state of charge (SoC) control, and components degradation in heavy-duty fuel cell vehicles. Ferrara et al. [17,18] propose model predictive control concepts using short-term driving forecasts to reduce fuel cell transients while retaining high system efficiency. Zendegan et al. [19] propose a dual-stage predictive energy management scheme based on the offline optimization of a predictive SoC reference, which is then used for the on-board control. In particular, the energy management problem is optimized using quadratic programming. The method uses long-term driving forecasts of speed and elevation to ensure that the battery is operated within the desired SoC range while retaining high system efficiency. Similar studies using predictive references for energy management can be found in Refs. [20–24]. Other works on optimal and heuristic energy management strategies for fuel cell electric vehicles can be found in Refs. [25–32].

The powertrain components sizing problem has also been a compelling topic in the research related to fuel cell electric vehicles. In the literature, it is widely acknowledged that components sizing must be coupled with optimal EMS design because the power-split criteria change depending on the powertrain configuration [33,34]. Jain et al. [35] use a genetic algorithm to optimize the parameters related to component sizing and load-follower charge sustaining EMS. The optimization considers a trade-off between fuel consumption and powertrain cost. Tazelaar et al. [36] use different EMSs for the optimal powertrain design showing that the minimum component size requirements are highly affected by the control strategy choice. Hu et al. [37] use convex programming for the combined optimization of energy management and component sizing, examining the influence of driving cycles on the optimization results. Xu et al. [34] investigate the optimal components sizing problem to find the best trade-off between consumption and degradation indicators, adopting an EMS based on dynamic programming. As follow-up work, Hu et al. [38] derive simplified EMSs from DP, showing that the hydrogen consumption is near-optimal if the battery capacity is large enough. Wu et al. [39] use convex programming for the combined optimization of energy management and component sizing of a plug-in fuel cell city bus, showing how the economic assumptions on the hydrogen price affect the energy management strategy. Fletcher et al. [40] use stochastic dynamic programming as EMS within their components sizing investigation, showing the impact of fuel cell size on the individual causes of degradation. Feng et al. [41] define an optimal components sizing problem to minimize the lifecycle

cost of a fuel cell mining truck, using simplified degradation models to estimate the component lifetime and, based on that, the total cost of ownership. Xu et al. [42] investigate the joint component sizing and energy management for fuel cell electric trucks proposing to decompose the problem into two sub-problems that are solved by sequential convex programming. Some works investigate the sizing problem on a higher system level through techno-economic assessments, neglecting or simplifying the role of energy management strategies [43–45].

Contribution

The present work focuses on the cost-optimal design and energy management of fuel cell electric trucks for road freight transport, investigating issues that have not been thoroughly addressed yet. In particular, the literature survey revealed the following research gaps.

- The cost-optimal design of fuel cell electric trucks has not been investigated to meet the high-performance requirements of road freight transport in challenging topographies (e.g. hilly or mountain roads).
- The combined impact on TCO of powertrain component sizing, driving cycle, vehicle weight, component degradation, and market prices has not been investigated for fuel cell electric trucks.
- The benefits of predictive energy management strategies for fuel cell electric trucks have not been analyzed in combination with powertrain component sizing.

To address the above-mentioned points, this paper proposes a cost optimization that relies on a novel predictive energy management scheme based on dynamic programming and the systematic calibration of control parameters to find the best trade-off between fuel consumption, components degradation, and battery charge control. In particular, the architecture of the predictive energy management system is divided into two control stages: route-reference optimization and on-board control, as proposed in Ref. [19]. However, an improved formulation is presented using dynamic programming for the multi-objective optimization of fuel consumption, SoC control, and fuel cell high-power operation prevention, which help reducing degradation.

The paper analyzes simulation results to highlight three main findings for fuel cell electric trucks.

1. Cost-optimal energy management is essential to define the best trade-off between fuel consumption and component degradation. The simulation results show that the control strategy significantly affects the TCO due to the high impact on system efficiency and lifetime. The contrasting behavior between fuel cell and battery life indicates that the EMS should be carefully designed to ensure balanced component degradation.
2. The total cost of ownership is significantly influenced by component sizing, driving cycles, vehicle weight, and market prices. In particular, the simulation results are analyzed for three real-world driving cycles (on flat, hilly, and mountain roads) and various truckload scenarios (from 18 to 40 tons). Moreover, it is shown that the

hydrogen price has a dominant influence on the TCO compared with the fuel cell and battery system prices.

3. Predictive energy management is highly beneficial in challenging road topographies for substantial cost-saving and lower component size requirements. In particular, the results show that non-predictive EMSs cannot meet high-performance requirements (for fuel consumption, vehicle lifetime, and battery charge control) on hilly or mountain roads.

The remainder of the paper is structured as follows. Section Total cost of ownership of fuel cell electric trucks outlines the simulation framework adopted to estimate the TCO of fuel cell electric trucks in realistic driving scenarios. Section Cost-optimal energy management describes the proposed predictive energy management system, detailing the methods adopted for the TCO optimization. Section Results of cost-optimal design and energy management analyzes the simulation results of the cost-optimal design and energy management. Section Conclusions concludes this work and outlines potential research directions.

Total cost of ownership of fuel cell electric trucks

The total cost of ownership assesses the long-term value of fuel cell electric trucks, considering the fixed and operating costs over their lifespan. A detailed TCO analysis includes direct and indirect costs of purchase, fuel, maintenance, insurance, downtime, repairs, fees, and taxes. However, this study only considers the purchase cost of the fuel cell and battery systems and the hydrogen cost, assuming that the impact of energy management and components sizing on the other costs is negligible.

Framework for TCO estimation

The total cost of ownership is estimated based on realistic simulations of fuel consumption and expected components life in fuel cell electric trucks for road freight transport. In particular, the TCO per unit distance (\$/km) is calculated as:

$$TCO = c_{H_2} SFC + \frac{c_{bat} E_{bat,nom} + c_{fcs} P_{fcs,nom}}{L_{veh}}, \quad (1)$$

where c_{H_2} is the hydrogen price, SFC the specific fuel consumption per unit distance, c_{bat} the battery system price, $E_{bat,nom}$ the nominal battery capacity, c_{fcs} the FCS price, $P_{fcs,nom}$ the nominal fuel cell power, and L_{veh} the vehicle life. It is assumed that the current market prices are 6 \$/kg for hydrogen [46], 40 \$/kW for fuel cell systems [47], and 160 \$/kWh for battery systems [48].

The specific fuel consumption, SFC, of the vehicle is calculated considering the total hydrogen consumption over the driving cycle and the equivalent battery consumption due to the SoC change compared to the initial charge:

$$SFC = \frac{\int_{dc} \dot{m}_{H_2} dt + \bar{\mu}_{H_2} E_{bat,nom} \Delta SoC}{L_{dc}}, \quad (2)$$

where \dot{m}_{H_2} is the hydrogen consumption rate, $\bar{\mu}_{H_2}$ is the fuel conversion factor (as in Ref. [17]), and L_{dc} is the distance traveled in the driving cycle.

The expected vehicle life is calculated assuming that the components cannot be replaced individually. Therefore, the vehicle life is over when one of the two power sources reaches the end-of-life conditions. Under this assumption, the vehicle life is calculated as:

$$L_{veh} = \min(L_{fcs}, L_{bat}) , \quad (3)$$

where L_{fcs} is the fuel cell system life and L_{bat} the battery system life, expressed in km. The component degradation over one driving cycle is projected to estimate the expected component life, assuming that the vehicle always repeats the same driving cycle with the same degradation. In particular, the fuel cell end-of-life occurs when the voltage degradation reaches 10%. Therefore, the fuel cell system life is estimated as:

$$L_{fcs} = \frac{\Delta V_{fcs, EoL}}{\Delta V_{fcs}} L_{dc} , \quad (4)$$

where $\Delta V_{fcs, EoL} = 10\%$, and ΔV_{fcs} is the fuel cell voltage degradation over the driving cycle, which is significantly affected by the energy management strategy. Similarly, the battery end-of-life life is estimated considering the number of equivalent full charge/discharge cycles (EFC), which are a measure of the battery current throughput over its lifespan. Therefore, the battery life is estimated as:

$$L_{bat} = \frac{EFC_{EoL}}{EFC} L_{dc} , \quad (5)$$

where $EFC_{EoL} = 5000$, assuming that the battery life can reach up to 5000 equivalent full cycles if the system is operated avoiding high C-rates and depth-of-discharge [49–53].

The vehicle simulation framework adopted in this work for obtaining realistic hydrogen consumption, fuel cell voltage degradation, and battery equivalent full cycles is described in.

Vehicle performance requirements

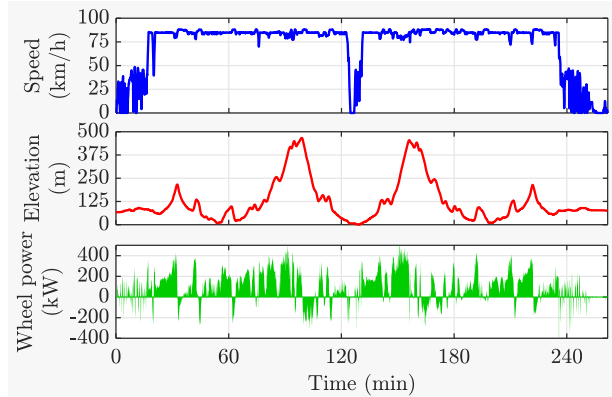
This study considers fuel cell electric trucks with high-performance requirements for fuel consumption, component degradation, and battery charge control. In particular, the vehicle performances are evaluated on driving cycles deriving from the real-world operation of conventional trucks in Europe. Indeed, it is essential that fuel cell electric trucks perform the same as conventional vehicles, especially at full truckload (i.e. 40 tons). Another critical requirement is imposed on the battery SoC, assuming that the following constraint must be met to ensure high vehicle performance:

$$0.45 \leq \text{SoC} \leq 0.85 . \quad (6)$$

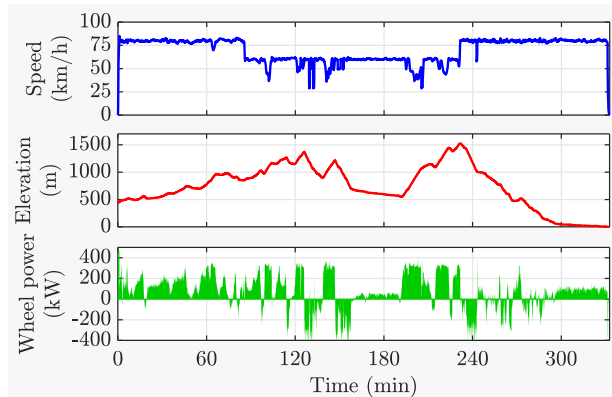
The values are defined to avoid accelerated degradation due to battery overcharging and critical discharging, which would weaken the assumption of 5000 EFC until end-of-life. Moreover, the SoC constraints are also essential to ensure that the battery always has enough charge to sustain the driving requirements (e.g. fast accelerations or route changes) but is never fully charged to perform regenerative braking consistently. For simplicity, it is assumed that the desired SoC

operating range in (6) does not change with the nominal battery capacity.

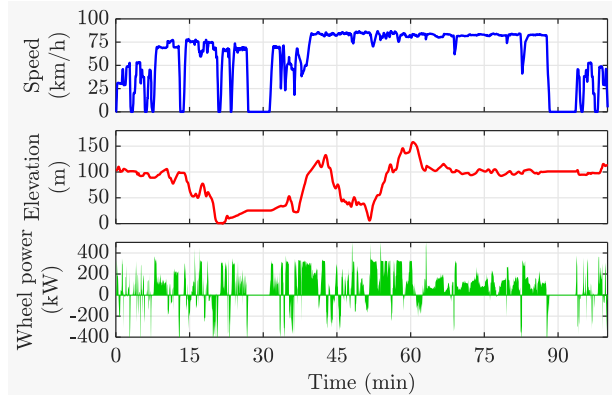
Three real-world driving cycles are selected to represent the diverse scenarios of flat, hilly, and mountain roads. The speed, elevation, and power at wheels (at full truckload: 40 tons) profiles of the three cycles are shown in Fig. 1. The speed profiles show that the first two cycles are motorway drives, whereas the third one is rural and includes traffic jams. The main characteristics of the real-world driving cycles under investigation are listed in Table 1. The rural drive on the flat



(a) driving cycle on hilly road



(b) driving cycle on mountain road



(c) driving cycle on flat road

Fig. 1 – Speed, elevation, and power at wheels (at full truckload: 40 tons) profiles of the three real-world driving cycles under investigation: a) hilly road, b) mountain road, and c) flat road.

Table 1 – Characteristics of the real-world driving cycles under investigation.

Route topography	hilly	mountain	flat
Elevation peak (m)	467	1530	158
Driving time (min)	262	333	100
Traveled distance (km)	316	385	100
Average speed (km/h)	72	69	60
RPA (m ² /s)	0.016	0.012	0.049
Average traction power (kW) ^a	118	112	110
Total traction energy (kWh) ^a	516	620	184
Specific traction energy (kWh/km) ^a	1.63	1.61	1.84

^a at full truckload (i.e. 40 tons).

route shows the highest relative positive acceleration (RPA) and specific traction energy due to frequent vehicle acceleration/deceleration maneuvers.

Cost-optimal energy management

The TCO optimization relies on a novel predictive energy management scheme based on dynamic programming and the systematic calibration of control parameters to find the best trade-off between fuel consumption, components degradation, and battery charge control. The predictive energy management system adopted in this work is divided into two control stages, as depicted in Fig. 2. In the route-references optimization stage, the electric load demand over the entire route is estimated based on the speed and elevation forecasts coming from the navigation system. Then, dynamic programming is used to calculate the optimal power split of the electric load between the fuel cell and battery systems to minimize the hydrogen consumption. The DP optimization results are distance-based maps of predictive SoC and FCS power references over the entire route. A rule-based energy management strategy then uses these references for the on-board control. The parameters of the rule-based strategy are calibrated to yield the cost-optimal trade-off between hydrogen consumption and expected vehicle life.

Dynamic programming for route-references optimization

The predictive energy management optimization problem is solved using dynamic programming. The implementation of DP requires discretization of the time, state, and input variables. However, one main difference from literature implementations is that the optimization problem under investigation is formulated over the traveled distance s instead of time t . Here, the distance is discretized in N elements with a uniform grid spacing: $\Delta s = 500$ m, which yields a good trade-off between accuracy and computational speed. The time interval to travel the distance Δs changes depending on the vehicle speed. Thus, the time interval for the k -th element is calculated as:

$$\Delta t_k = \Delta s / v_k \quad (7)$$

For clarity, the problem is formulated using the notation of optimal control theory [54]. In (8), x represents the state variable, u the input, and z the disturbance.

$$x = \text{SoC}, \quad u = P_{fcs}, \quad z = P_{el} \quad (8)$$

Due to the discretization requirements, the electric load in the k -th element is the average over the time interval Δt_k . Considering (A.5), the state dynamics are a function of x , u , and z as follows:

$$\dot{x} = f(x, u, z) = -\frac{V_{oc}(x) - \sqrt{V_{oc}^2(x) - 4(z - u) R_{int}(x)}}{2 Q_{nom} R_{int}(x)} \quad (9)$$

In general, it is not straightforward to implement the expected TCO as the objective function of dynamic programming as it is a highly complex problem. Moreover, the component degradation is highly sensitive to load fluctuations, which cannot be accurately forecasted. Therefore, this work optimizes the predictive energy management references, considering fuel consumption as the main target. In particular, the hydrogen consumption rate is defined in (10) as the stage cost L in the objective function. Under this assumption, the cost function depends only on the input variable.

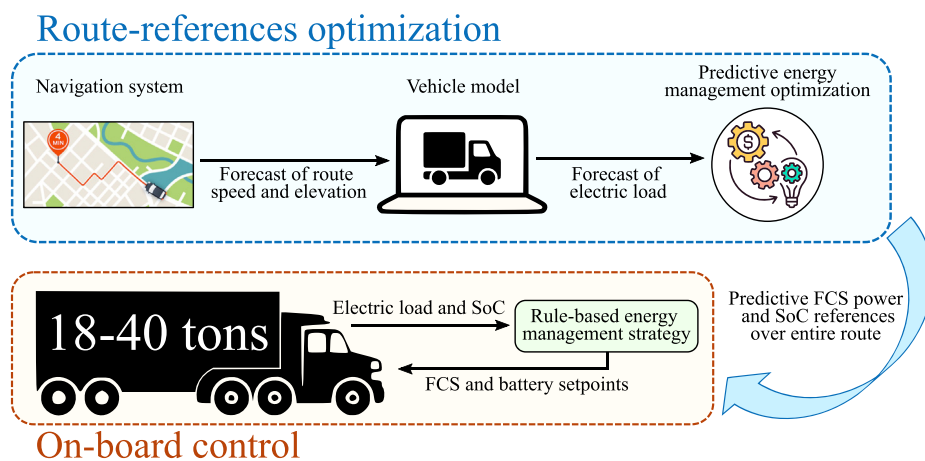


Fig. 2 – The predictive energy management architecture is divided into two control stages: route-references optimization and on-board control.

$$L(u) = \dot{m}_{H_2} \quad (10)$$

Soft constraints on the battery state of charge and fuel cell power are included in the objective function through the penalty φ defined in (11), where $L_{max} = L(u_{max})$. In particular, the battery operation outside the 50–80% SoC range is highly penalized. Moreover, a penalty is active above 80% of the nominal power to avoid the fuel cell high power operation.

$$\varphi(x, u) = \begin{cases} 10 \cdot L_{max} & \text{if } x < 0.50 \text{ or } x > 0.80 \\ L_{max} & \text{if } u > 0.80 P_{fcs,max} \\ 0 & \text{otherwise} \end{cases} \quad (11)$$

Eventually, the optimization problem is defined in (12). The objective function J is the sum of the stage cost L and the penalty function φ over the entire trip.

$$\min_{\{u_1, u_2, \dots, u_N\}} J = \sum_{k=1}^N [L(u_k) + \varphi(x_k, u_k)] \Delta t_k \quad (12a)$$

subject to:

$$x_{k+1} = x_k + f(x_k, u_k, z_k) \Delta t_k \quad (12b)$$

$$x_1 = x_N = 0.65 \quad (12c)$$

$$0.45 \leq x_k \leq 0.85 \quad (12d)$$

$$P_{fcs,min} \leq u_k \leq P_{fcs,max} \quad (12e)$$

$$P_{bat,min} \leq z_k - u_k \leq P_{bat,max} \quad (12f)$$

The initial and terminal SoC are set equal in (12c) to ensure the battery charge sustaining. Hard constraints are implemented in (12d) for the SoC, in (12e) for the fuel cell power, and in (12f) for the battery power. The DP solution is found by setting the number of grid elements for the state and input variable discretization to 900 and 100, respectively, which yield a good trade-off between accuracy and computational speed (i.e. a few seconds). The resulting predictive SoC and FCS power references are stored as distance-based maps over the entire route. The references are denoted with SoC_{ref} and $P_{fcs,ref}$, respectively.

It should be mentioned that this work neglects prediction uncertainties and assumes that the speed forecast of the navigation system is exact. This assumption is reasonable, considering that the scope of the investigation is to analyze the potential benefits of predictive energy management based on system-level simulation results. Moreover, the results in Ref. [19] show a low sensitivity of uncertain predictions for fuel consumption optimization.

Rule-based EMS for on-board control

The electric load request coming from the driver, P_{el}^* , is split between the fuel cell and battery systems by a rule-based energy management strategy. The fuel cell power setpoint, P_{fcs}^* , is defined following the rules in (13).

$$P_{fcs}^* = P_0 + r_1 (P_{el}^* - P_0) + r_2 (SoC_{ref} - SoC) E_{bat,nom} \quad (13a)$$

subject to:

$$P_{el}^* - P_{fcs}^* \leq P_{bat,max} \quad (13b)$$

$$|P_{fcs}^*| \leq r_3 P_{fcs,nom} \quad (13c)$$

$$r_4 P_{fcs,nom} \leq P_{fcs}^* \leq P_{fcs,nom} \quad (13d)$$

$$\text{if } r_5 = 0, \text{ then : } P_{el}^* - P_{fcs}^* \geq P_{bat,min} \quad (13e)$$

$$P_0 = \begin{cases} P_{fcs,ref} & \text{if } r_6 = 1 \\ P_{fcs,opt} & \text{if } r_6 = 0 \end{cases} \quad (13f)$$

In (13b), the setpoint is constrained to consider the battery maximum power limit. Whereas in (13c), the rate of change of the setpoint is limited. Equation (13d) defines the lower limit for the setpoint. In (13e), the fuel cell power is constrained to consider the battery minimum power limit. However, this constraint is active only if r_5 is zero. Lastly, depending on the value of r_6 , the EMS considers in (13f) the predictive FCS reference or the optimal fuel cell operating point. The first case generally yields closer tracking of the predictive SoC reference, whereas the second results in lower hydrogen consumption and poorer SoC control. The battery setpoint, P_{bat}^* , is defined as:

$$P_{bat}^* = P_{el}^* - P_{fcs} \eta_{dc/dc}(P_{fcs}) \quad (14)$$

Here, the battery acts as a buffer between the fuel cell system and the electric loads. Details about the efficiency of the fuel cell DC/DC converter, $\eta_{dc/dc}$, are provided in Appendix A.

The EMS parameters in (13) have a significant impact on the overall vehicle performance and total cost of ownership. Eventually, for cost-optimal energy management, it is necessary to find the set of parameters that yields the minimum TCO, which generally changes depending on the powertrain configuration and driving cycle. Therefore, it is essential to establish a method to properly tune the control strategy and find the cost-optimal EMS for each powertrain configuration and driving cycle. To this end, using a design of experiment (DoE) strategy is a practical method to calibrate the EMS parameters systematically. In particular, this work uses Latin hypercube sampling [55] to generate 2000 combinations of the six parameters and explore the entire calibration design space. Eventually, the expected TCO is evaluated for the 2000 parameter combinations to find the cost-optimal EMS for each driving cycle and powertrain configuration. Besides the TCO, this work also considers the SFC, L_{fcs} , L_{bat} , L_{veh} , SoC_{min} , and SoC_{max} as key performance indicators (KPIs). The variation ranges of the individual parameters are defined in Table 2.

Table 2 – DoE variation range for Latin hypercube sampling of EMS parameters.

r_1	r_2	r_3	r_4	r_5	r_6
[0, 1]	[5e3, 1e5]	[0.03, 0.10]	{0, 0.1}	{0, 1}	{0, 1}

Results of cost-optimal design and energy management

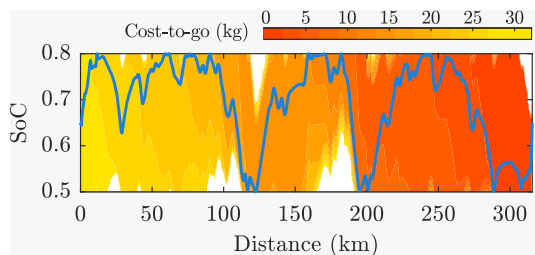
This section examines the results of cost-optimal design and energy management, and the impact of the key influencing factors on the total cost of ownership. The investigation considers powertrain configurations with fuel cell nominal power ranging between 200 kW and 400 kW, and nominal battery capacity between 40 kWh and 160 kWh. The higher limits of this design space are defined considering the practical packaging of the components in the vehicle, whereas the lower limits are defined to meet the driving performance requirements. The tuning yielding the minimum TCO is found as described in Section Cost-optimal energy management for each powertrain configuration and driving cycle.

Analysis of energy management results

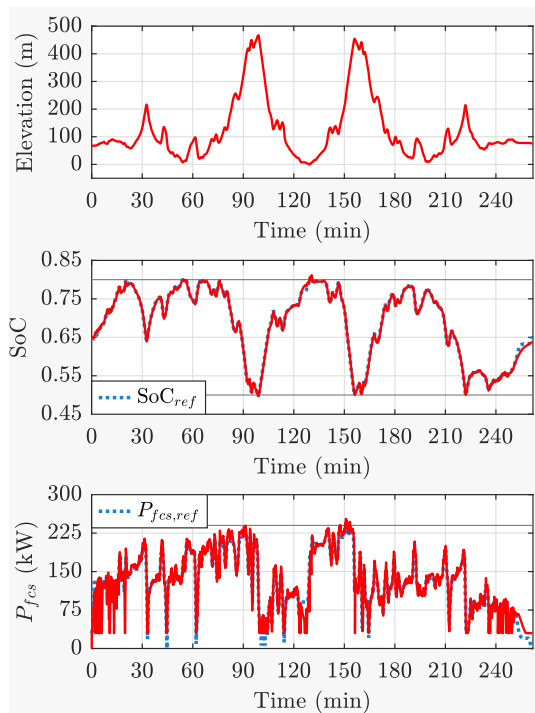
Fig. 3 collects the results of the cost-optimal energy management proposed in Section Cost-optimal energy management

for a fixed powertrain configuration, the hilly road driving cycle, and 40-tons base vehicle weight.

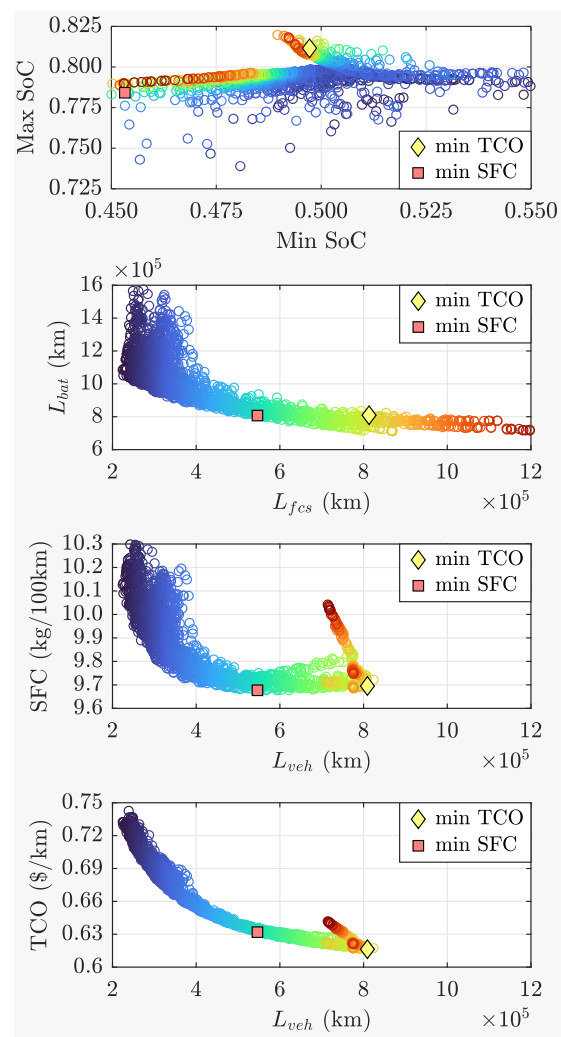
- Fig. 3a shows the DP optimization results in terms of the optimal SoC trajectory and the cost-to-go J (12), which is the cost from any point of the distance-SoC space to reach the terminal SoC target. Notably, the SoC stays within the desired range thanks to the soft-constraints in the penalty function (11). The white spaces in the cost-to-go map are the infeasible areas that would determine violations of the SoC constraints (6).
- Fig. 3b shows the on-board control results using the rule-based EMS to follow the optimal references created with DP. The close tracking of the predictive references demonstrates the benefits for SoC control and avoiding high FCS power operation. In particular, before the long uphill, the predictive EMS ensures that the battery is fully charged (i.e. to the desired maximum SoC).
- Fig. 3c shows the simulation results for the 2000 EMS tuning variations explored in the calibration process. The figure highlights the contrasting relationship



(a) DP results for route-references optimization.



(b) On-board control results for minimum TCO.



(c) Impact of EMS parameters calibration on KPIs.

Fig. 3 – Results of cost-optimal energy management for a fixed powertrain configuration ($P_{fcs,nom} = 300$ kW and $E_{bat,nom} = 100$ kWh), considering the hilly road driving cycle.

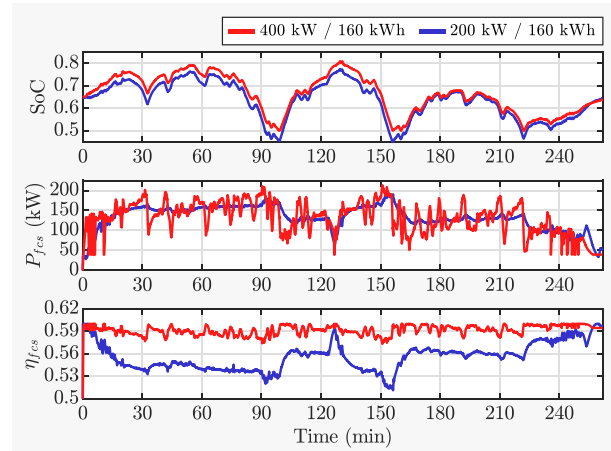
between the main KPIs and indicates the tunings corresponding to the minimum TCO and SFC. First, the minimum and maximum SoC provide meaningful information on the battery operation and charge control. The second tile shows the contrast between the fuel cell and battery life expectations, indicating that it is not possible to maximize the life of both components at the same time. The third tile shows the trade-off between fuel consumption and vehicle life. The extreme cases of high battery life (in blue) and fuel cell life (in red) can only be achieved with a significant increase in hydrogen consumption. On the other hand, the vehicle life can be significantly extended with a tiny increase ($\sim 0.2\%$) of fuel consumption compared to the minimum value. Lastly, the bottom tile shows that energy management significantly impacts the TCO. Moreover, the tuning for minimum SFC determines a 2.6% higher TCO compared to the optimal value. Therefore, it is essential to consider the suitable trade-off between vehicle life and fuel consumption to obtain a cost-optimal EMS design.

Fig. 4 compares the cost-optimal EMS for some extreme cases of powertrain configurations to show examples of how the optimal control strategy changes depending on the component sizes. In particular, Fig. 4a compares two configurations with the same battery capacity but different nominal fuel cell power: i.e. 400 kW and 200 kW. There are two main differences. Firstly, even if the fuel cell power is similar, the fuel cell efficiency is significantly higher for the 400 kW system. Secondly, the cost-optimal EMS operates the smaller fuel cell system in a stationary way to minimize the fuel cell voltage degradation due to dynamic loading. Such operation is obtained when the constraint (13d) is not active (i.e. $r_5 = 0$). In this case, the fuel cell power is not reduced during regenerative braking, leading to energy waste in mechanical brakes. Therefore, the vehicle with the larger FCS has a significantly lower fuel consumption (see Fig. 4c) because of higher efficiency and braking energy regeneration. Moreover, the vehicle with smaller FCS shows unbalanced component degradation because the cost-optimal EMS corresponds to the one that maximizes the fuel cell life. Instead, the other configuration uses the fuel cell more dynamically to balance the degradation with the battery system.

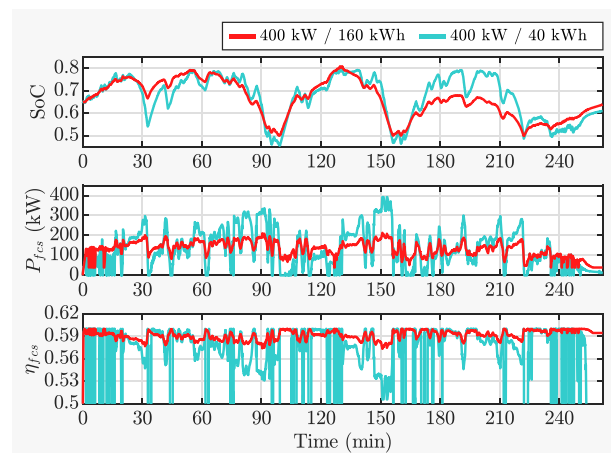
On the other hand, Fig. 4b compares two configurations with the same nominal fuel cell power but different nominal battery capacity: i.e. 160 kWh and 40 kWh. In the second configuration, where there is a slight degree of freedom due to the low battery capacity, the EMS must operate in a broader fuel cell power range to meet the battery SoC constraints. Such an operating strategy results in lower FCS efficiency and life. Eventually, the comparison of the key performance indicators in Fig. 4c shows that the powertrain with larger fuel cell and battery systems has an 8% lower TCO than the other two cases.

Impact on TCO of driving cycles and component sizing

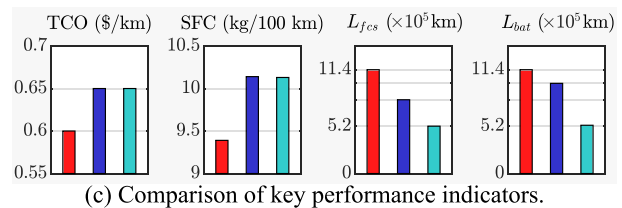
Fig. 5 shows the impact on TCO of fuel cell and battery sizes for the three driving cycles under investigation, with a base vehicle weight of 40 tons. The contour lines delimit a 2%



(a) Impact of fuel cell system size.



(b) Impact of battery system size.



(c) Comparison of key performance indicators.

Fig. 4 – Comparison of fuel cell and battery operation for different powertrain configurations.

increment compared to the minimum TCO (blue cross marker), showing a large impact of component sizing on the total cost of ownership. The minimum TCO is at 160 kWh of nominal battery capacity in all cycles. On the other hand, the optimal nominal FCS power is 400 kW in Fig. 5a and 350 kW in Fig. 5b, and 300 kW in Fig. 5c, indicating that the FCS efficiency and life improvement do not compensate for the higher component weight and cost. The figure also shows the powertrain requirements to avoid SoC constraint (6) violations, indicating why it is critical to consider hilly and mountain driving cycles for the design of fuel cell electric trucks. In particular, the lower the FCS size, the higher the battery requirement is. In Fig. 5c, the TCO is higher than the others because of the frequent accelerations of the flat road driving cycle (see Fig. 1c), resulting in higher specific traction energy (see Fig. 1c) and, thus, SFC.

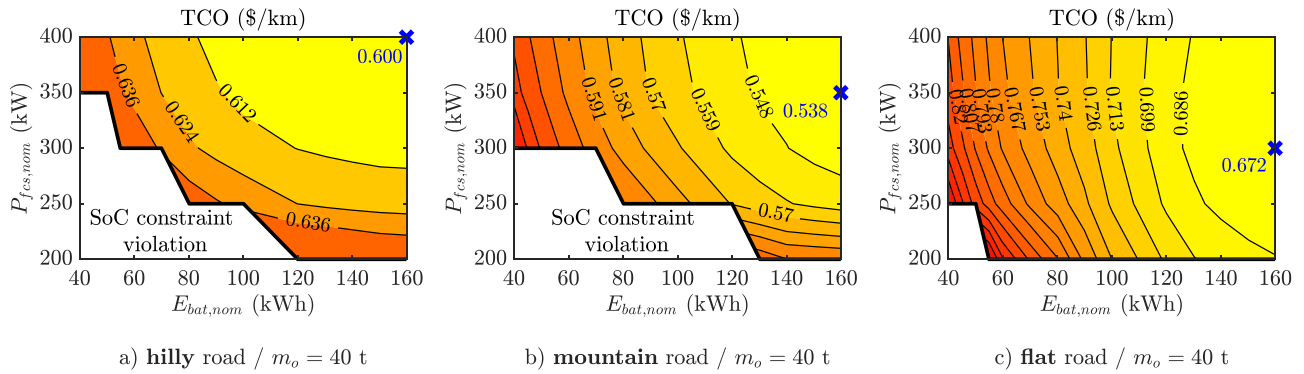


Fig. 5 – Impact of powertrain component sizing on TCO for different driving cycles and 40 tons base vehicle weight. The contour lines delimit a 2% increment compared to the minimum value (blue cross marker). (For interpretation of the references to color in this figure legend, the reader is referred to the Web version of this article.)

Impact on TCO of truckload and component sizing

Fig. 6 shows the impact on TCO of different truckloads and component sizing, considering the hilly road driving cycle. The contour lines delimit a 1% increment compared to the minimum TCO. Fig. 6a shows a low TCO sensitivity to the powertrain configuration for a base vehicle weight of 18 tons (i.e. no truckload). Moreover, the minimum TCO is at the configuration: 300 kW/80 kWh. The other sub-figures indicate that the higher truckload, the higher the powertrain requirements and the TCO sensitivity to the configuration. Fig. 6f shows the TCO for a combined driving cycle, which is obtained by averaging the fuel consumption and degradation

of the five truckloads. In this case, the minimum TCO is at a lower battery size compared to the full truckload case. However, Fig. 6f also shows that several configurations determine a TCO that is within a 1% deviation from the minimum value.

Two powertrain configurations are selected for a quantitative comparison of the TCO, SFC, and vehicle life. Configuration A is 400 kW/130 kWh, which corresponds to the minimum TCO in Fig. 6f. Configuration B is 300 kW/100 kWh, which is within a 1% deviation from the minimum TCO in Fig. 6f. Table 3 lists the results for all the cases considered in Figs. 5 and 6. Overall, configuration A shows lower TCO than B, with the largest deviations for the cycles with 40 tons of vehicle weight. The table shows the significant truckload

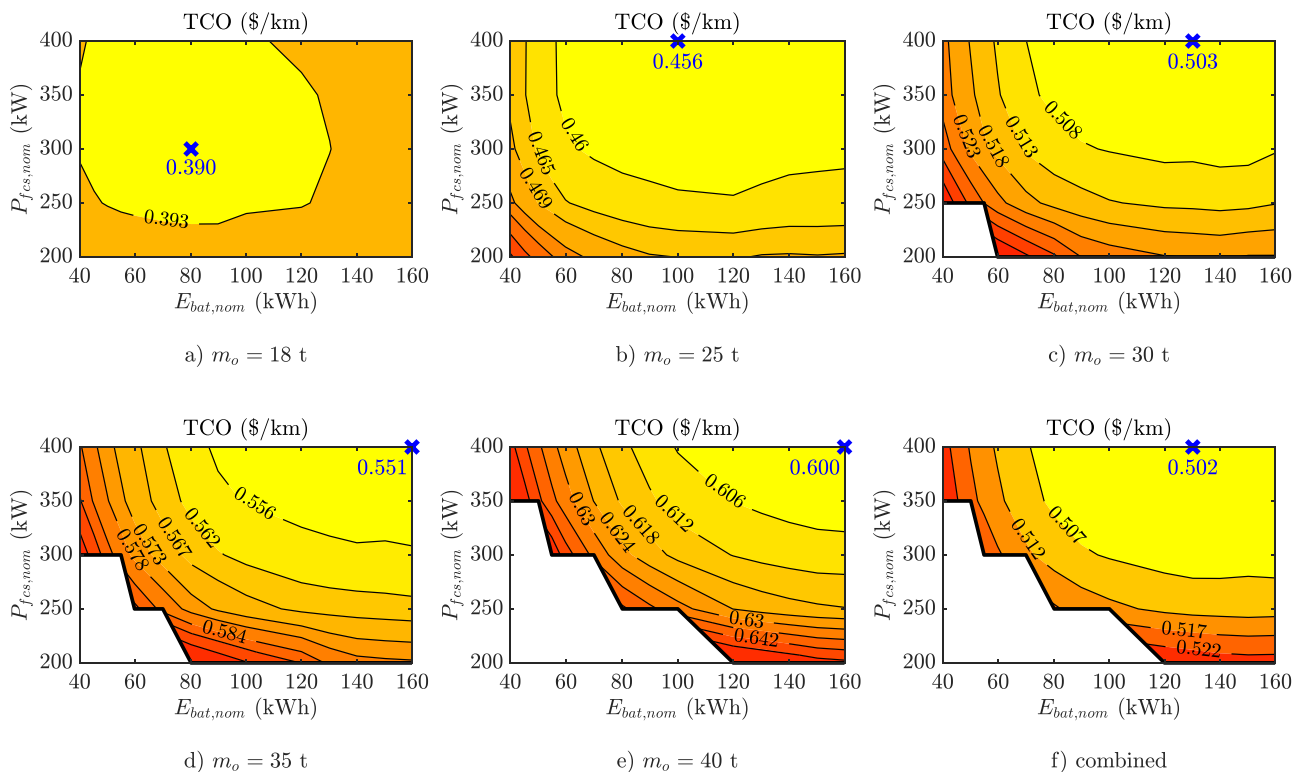


Fig. 6 – Impact of powertrain component sizing on TCO for different base vehicle weights on the hilly road driving cycle. The contour lines delimit a 1% increment compared to the minimum value (blue cross marker). (For interpretation of the references to color in this figure legend, the reader is referred to the Web version of this article.)

Table 3 – Impact of truckload and driving cycles on TCO, SFC, and vehicle life for two selected powertrain configurations.

Cycle/weight	TCO (\$/km)		SFC (kg/100 km)		L_{veh} ($\times 10^5$ km)	
	A	B	A	B	A	B
hilly combined	0.502	0.507	7.86	7.98	12.8	10.2
18 t	0.395	0.391	6.18	6.18	15.5	13.8
25 t	0.458	0.457	7.18	7.21	13.5	11.4
30 t	0.503	0.508	7.89	7.99	12.5	9.99
35 t	0.552	0.560	8.63	8.83	11.0	9.13
40 t	0.601	0.616	9.41	9.70	9.97	8.09
mountain/40 t	0.546	0.571	8.45	8.90	9.52	7.59
flat/40 t	0.685	0.716	10.20	10.95	4.92	4.74

Powertrain configuration A: 400 kW/130 kWh
Powertrain configuration B: 300 kW/100 kWh

impact on the SFC and vehicle life, and configuration A always has better results for these KPIs. Lastly, the expected vehicle life for the driving cycle on the flat road is lower because of the

shorter traveled distance (see Table 1). Indeed, if the truck always repeats this driving cycle, there will be a much higher voltage degradation due to the start-up/shut-down cycles.

Impact on TCO of market prices

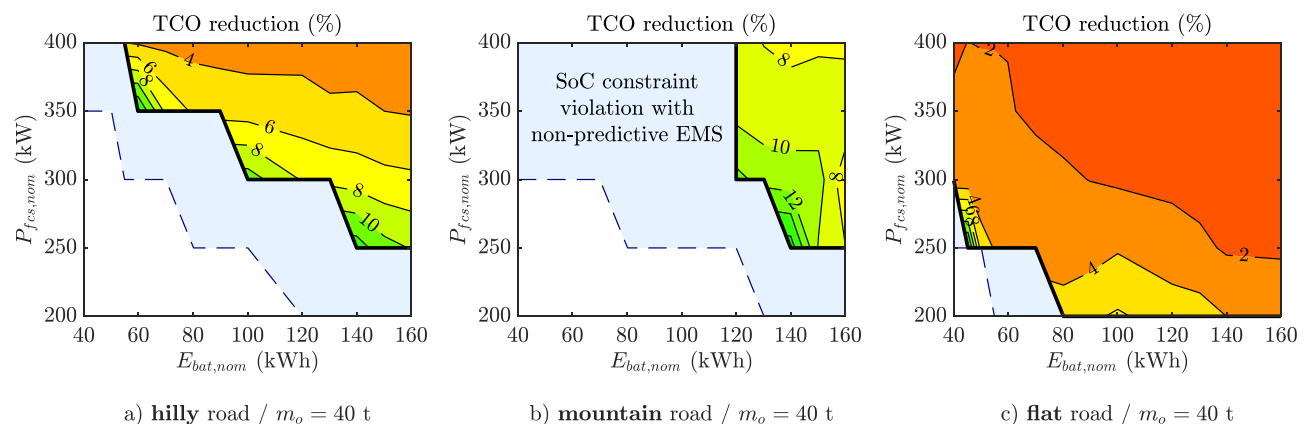
The market prices of hydrogen, fuel cell, and battery systems significantly affect the TCO. Table 4 shows the results for the combined driving cycle (see Fig. 6f) for different combinations of market prices, showing the optimal TCO and powertrain configuration, and the TCO deviation of configurations A and B from the optimal one. The market prices adopted so far are reported in bold characters. The table indicates that the hydrogen price has a much higher impact on the TCO than the fuel cell and battery prices. In most cases, configuration A is optimal and the highest deviation (i.e. 1.3%) results from the scenario in which the hydrogen is rather cheap and the powertrain expensive.

The second half of Table 4 shows the extreme scenarios in which either the powertrain or hydrogen price is zero. In the

Table 4 – Impact of market prices on TCO and optimal configuration.

Market prices			Optimal configuration			TCO dev. (%)	
C_{H_2}	C_{fcs}	C_{bat}	$P_{fcs,nom}$	$E_{bat,nom}$	TCO	A	B
(\$/kg)	(\$/kW)	(\$/kWh)	(kW)	(kWh)	(\$/km)		
2	20	80	400	120	0.172	0.0	0.8
2	40	160	350	140	0.187	0.3	0.3
2	80	320	300	120	0.214	1.3	0.1
6	20	80	400	130	0.486	–	1.2
6	40	160	400	130	0.502	–	1.0
6	80	320	350	140	0.531	0.1	0.6
10	20	80	400	130	0.800	–	1.4
10	40	160	400	130	0.816	–	1.2
10	80	320	400	130	0.846	–	0.9
2	0	0	400	130	0.157	–	1.6
6	0	0	400	130	0.471	–	1.6
10	0	0	400	130	0.785	–	1.6
0	20	80	250	130	0.013	13.3	3.7
0	40	160	250	130	0.026	13.3	3.7
0	80	320	250	130	0.053	13.3	3.7

Powertrain configuration A: 400 kW/130 kWh
Powertrain configuration B: 300 kW/100 kWh

**Fig. 7 – TCO reduction using the predictive EMS compared to the non-predictive, considering different powertrain component sizes and driving cycles.**

first case, the optimal configuration is the one that minimizes the SFC, whereas, in the second one, it is the one that maximizes the vehicle life.

Benefits of predictive energy management

This paper also investigates the benefits of predictive EMSs compared to non-predictive ones regarding TCO improvement and reduction of powertrain component size requirements. The rule-based control strategy described in Section Rule-based EMS for on-board control is adopted for non-predictive energy management using a constant SoC reference of 65% and $r_6 = 0$. For a fair comparison, the tuning yielding the minimum TCO is found for each powertrain configuration using the same calibration procedure described in Section Rule-based EMS for on-board control. Fig. 7 shows the TCO reduction using predictive EMSs instead of non-predictive ones for the three driving cycles with $m_o = 40$ t. The TCO reduction is significant for the hilly and mountain driving cycles, whereas much lower for the flat one. The light blue area indicates valid configurations with predictive EMSs and invalid with non-predictive ones because they cannot meet the SoC constraints. Therefore, the component size requirements are significantly reduced using predictive energy management to improve the SoC control.

Conclusions

This paper investigated the cost-optimal design and energy management of fuel cell electric trucks for road freight transport. A novel predictive energy management system based on dynamic programming was proposed for the multi-objective optimization of SoC control, fuel consumption, and expected components life. The significant impact of energy management on the total cost of ownership and the other key performance indicators highlights the critical role of this supervisory control function. It is shown that the cost-optimal EMS is essential to define the best trade-off between fuel consumption and component degradation, leading to significantly lower TCO than the fuel-optimal EMS.

The paper highlights that component sizing, driving cycles, truckload, and market prices significantly influence the cost-optimal design and energy management. The powertrain component size requirements were defined in challenging driving cycles considering hilly and mountain roads at full truckload. Some selected configurations are analyzed in detail to show that the fuel cell and battery sizes significantly affect the power-split strategy and the vehicle performance. Moreover, it is shown that the hydrogen price has a dominant impact on the TCO compared to the fuel cell and battery prices. However, the optimal powertrain configuration shows low sensitivity to the market prices.

The study also demonstrated the benefits of predictive energy management for TCO improvement and reduction of powertrain component size requirements. The benefits are particularly evident in challenging driving cycles (due to road topographies and full truckload), both for cost-saving and lower component size requirements.

A potential research direction for future investigations is to formulate the expected TCO as the objective function of dynamic programming. Additionally, it will be essential to increase the robustness of the vehicle design by including more driving cycles and truckload scenarios, and speed uncertainties within the electric load forecasting system. Moreover, a limiting assumption of the present work is that the fuel cell and battery degradation over one driving cycle is projected to estimate the component life, assuming that its characteristics do not change with degradation. Overcoming these limitations opens an additional research direction: a health-conscious EMS to maintain a balanced degradation between the fuel cell and battery systems.

Declaration of competing interest

The authors declare that they have no known competing financial interests or personal relationships that could have appeared to influence the work reported in this paper.

Acknowledgments

The financial support by the Austrian Federal Ministry for Digital and Economic Affairs, the National Foundation for Research, Technology and Development, TU Wien Bibliothek, and the Christian Doppler Research Association is gratefully acknowledged. This work has been created in cooperation with the Austrian research projects “HyTruck” (grant no. 868790) and “FC4HD” (grant no. 885044).

Appendix A. Vehicle simulation framework

This section describes the vehicle simulation framework adopted for a realistic estimation of fuel consumption and component degradation in fuel cell electric trucks. The architecture of the electric powertrain is equivalent to the one shown in Ref. [17]. The simulation models are scalable to analyze the vehicle performance for powertrain configurations with nominal fuel cell power ranging between 200 kW and 400 kW, and nominal battery capacity between 40 kWh and 160 kWh. The simulation framework is implemented in MATLAB/Simulink with a structure similar to the one reported in Ref. [56].

Appendix A.1. Fuel cell vehicle modeling

The vehicle modeling approach is forward-facing, including a driver model that generates a load request based on the deviation from the target speed depicted in Fig. 1. According to this modeling approach, the vehicle slows down if the powertrain does not provide the requested power. The vehicle acceleration \dot{v} is calculated as in depending on the vehicle speed v , road slope α , fuel cell system power P_{fcs} , and battery power P_{bat} .

$$m_v \dot{v} = P_w/v - F_{res} \quad (\text{A.1a})$$

$$F_{res} = v^2 A_v c_x \rho_{air} / 2 + m_v g (c_r \cos \alpha + \sin \alpha) \quad (A.1b)$$

$$P_w = P_m \eta_T^{sgn(P_m)} - P_{br} \quad (A.1c)$$

$$P_m = P_{el} - P_{aux} \quad (A.1d)$$

$$P_{el} = P_{fcs} \eta_{dc/dc}(P_{fcs}) + P_{bat} \quad (A.1e)$$

The mechanical braking power, P_{br} , compensates for the power request that cannot be absorbed as regenerative braking energy. The vehicle dynamics parameters are reported in. In particular, the rolling friction coefficient c_r in (A.1b) changes linearly with the vehicle speed. Moreover, the vehicle mass is calculated depending on the powertrain components size as:

$$m_v = m_o + \mu_{fcs} P_{fcs,nom} + \mu_{bat} E_{bat,nom} \quad (A.2)$$

The converter efficiency in (A.1e) depends on the FCS power as depicted in Figure A.8. The hydrogen consumption rate is calculated as:

$$\dot{m}_{H_2} = P_{fcs} / (\eta_{fcs} LHV_{H_2}), \quad (A.3)$$

where η_{fcs} is the FCS efficiency with the characteristic depicted in Figure A.8 as a function of the normalized fuel cell power. In general, it is not possible to directly scale the characteristics of fuel cell systems to a different size because increasing the number of cells can cause the non-uniform distribution of reactants and might determine changes in the auxiliary component requirements. However, this work assumes for simplicity that the efficiency curve can be scaled only based on the nominal fuel cell power. The hydrogen consumption rate is used in (2) to calculate the specific fuel consumption.

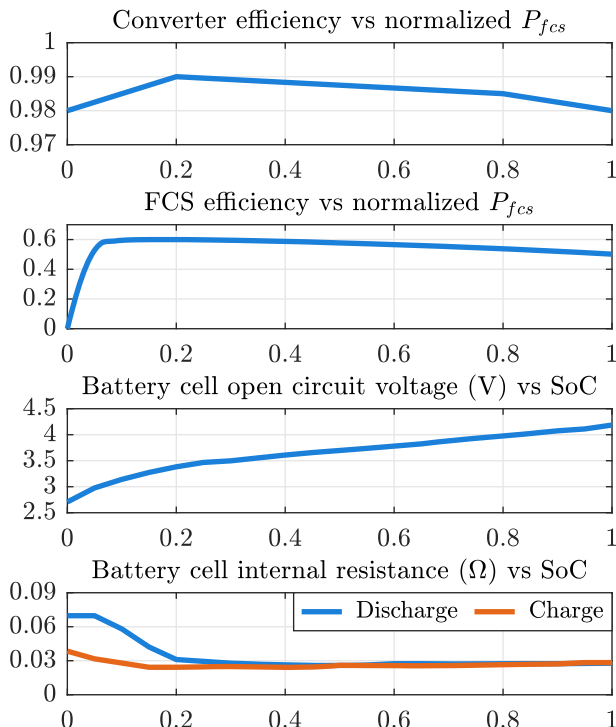


Figure A.8 – Characteristics of DC/DC converter, fuel cell system, and battery cell.

The open-circuit voltage, internal resistance, nominal charge, and nominal capacity of the battery cell are scaled to the whole battery pack as in (A.4), where N_p is the number of parallel branches, each of which has N_s cells connected in series.

$$V_{oc} = V_{oc,cell} N_s \quad (A.4a)$$

$$R_{int} = R_{int,cell} N_s / N_p \quad (A.4b)$$

$$Q_{nom} = Q_{nom,cell} N_p \quad (A.4c)$$

$$E_{bat,nom} = E_{nom,cell} N_s N_p \quad (A.4d)$$

The battery cell open-circuit voltage and internal resistance depend on the SoC as depicted in Figure A.8, whereas the impact of the temperature is neglected. The cell nominal charge and capacity are reported in Table A.5. The SoC rate of change is calculated as a function of the battery power:

$$\frac{d}{dt} \text{SoC} = -\frac{V_{oc} - \sqrt{V_{oc}^2 - 4 P_{bat} R_{int}}}{2 Q_{nom} R_{int}}, \quad (A.5)$$

adopting the equivalent circuit model described in Ref. [17]. The fuel cell system is subject to the power constraints:

$$0 \leq P_{fcs} \leq P_{fcs,nom} \quad (A.6a)$$

$$|\dot{P}_{fcs}| \leq 0.10 P_{fcs,nom} \quad (A.6b)$$

where the rate of change is limited to the 10% of the nominal power per second. The battery power is constrained to meet the cell voltage and C-rate limits:

$$2.6 \leq V_{cell} \leq 4.2 \quad (A.7a)$$

$$-2 \leq C - \text{rate} \leq 8 \quad (A.7b)$$

which ensure a battery operation without accelerated degradation.

Table A.5: Vehicle model parameters.

Parameter	Symbol	Value
Friction coefficient at 0 km/h	c_r	0.0055
Friction coefficient at 100 km/h	c_r	0.0081
Vehicle frontal area	A_v	9.6 m ²
Drag coefficient	c_x	0.58
Auxiliary loads	P_{aux}	11.5 kW
Total efficiency	η_T	0.87
Base vehicle mass	m_o	40 t
Specific FCS weight	μ_{fcs}	1.27 kg/kW
Specific battery weight	μ_{bat}	6.35 kg/kWh
Hydrogen lower heating value	LHV _{H₂}	120 MJ/kg
Nominal cell charge	$Q_{nom, cell}$	2.7 Ah
Nominal cell capacity	$E_{nom, cell}$	9.72 Wh

Appendix A.2. Fuel cell and battery degradation models

The quick evaluating method for fuel cell voltage degradation developed by Pei et al. [57] has been used in several

works to assess the impact of energy management strategies on fuel cell life [58–61]. This method derives from accelerated aging tests and offers adequate precision for a system-level analysis. In particular, the voltage degradation of the fuel cell system is estimated using the formula in (A.8), considering start-up/shut-down cycles (*ss*), low-power operation time (*lp*), high-power operation time (*hp*), and dynamic loading (*dl*).

$$\Delta V_{fcs} = \Delta V_{fcs,ss} + \Delta V_{fcs,lp} + \Delta V_{fcs,hp} + \Delta V_{fcs,dl} \quad (\text{A.8a})$$

$$\Delta V_{fcs,ss} = 0.00196 \cdot N_{starts} \quad (\text{A.8b})$$

$$\Delta V_{fcs,lp} = 0.00126 \cdot t_{lp} \quad (\text{A.8c})$$

$$\Delta V_{fcs,hp} = 0.00147 \cdot t_{hp} \quad (\text{A.8d})$$

$$\Delta V_{fcs,dl} = 0.0000593 \cdot \int_{dc} |\dot{P}_{fcs} / P_{fcs,nom} / 2| dt \quad (\text{A.8e})$$

The thresholds for low and high-power operation are assumed as 10% and 80% of the fuel cell nominal power, as in Ref. [58]. The total voltage degradation ΔV_{fcs} over each driving cycle (*dc*) is expressed in percentage compared to the begin-of-life conditions. The voltage degradation is used in (4) to calculate the fuel cell system life.

Battery degradation mechanisms are highly specific to the cell type, making it challenging to generalize degradation models. However, an important indicator for battery life is the number of equivalent full charge/discharge cycles:

$$EFC = \frac{\int_{dc} |I_{bat}| dt}{2 Q_{bat,nom}} \quad (\text{A.9})$$

This work assumes that the battery pack load is equally distributed among its cells. Eventually, the EFC is used in (5) to calculate the battery system life.

REFERENCES

- [1] Lee D-Y, Elgowainy A, Kotz A, Vijayagopal R, Marcinkoski J. Life-cycle implications of hydrogen fuel cell electric vehicle technology for medium- and heavy-duty trucks. *J Power Sources* 2018;393:217–29. <https://doi.org/10.1016/j.jpowsour.2018.05.012>.
- [2] Kast J, Vijayagopal R, Gangloff JJ, Marcinkoski J. Clean commercial transportation: medium and heavy duty fuel cell electric trucks. *Int J Hydrogen Energy* 2017;42(7):4508–17. <https://doi.org/10.1016/j.ijhydene.2016.12.129>.
- [3] Liu F, Zhao F, Liu Z, Hao H. The impact of fuel cell vehicle deployment on road transport greenhouse gas emissions: the China case. *Int J Hydrogen Energy* 2018;43(50):22604–21. <https://doi.org/10.1016/j.ijhydene.2018.10.088>.
- [4] Enang W, Bannister C. Modelling and control of hybrid electric vehicles (a comprehensive review). *Renew Sustain Energy Rev* 2017;74:1210–39. <https://doi.org/10.1016/j.rser.2017.01.075>.
- [5] Lü X, Wu Y, Lian J, Zhang Y, Chen C, Wang P, Meng L. Energy management of hybrid electric vehicles: a review of energy optimization of fuel cell hybrid power system based on genetic algorithm. *Energy Convers Manag* 2020;205:112474. <https://doi.org/10.1016/j.enconman.2020.112474>.
- [6] Teng T, Zhang X, Dong H, Xue Q. A comprehensive review of energy management optimization strategies for fuel cell passenger vehicle. *Int J Hydrogen Energy* Feb. 2020. <https://doi.org/10.1016/j.ijhydene.2019.12.202>.
- [7] Kandidayeni M, Trovão J, Soleymani M, Boulon L. Towards health-aware energy management strategies in fuel cell hybrid electric vehicles: a review. *Int J Hydrogen Energy* 2022;47(17):10021–43. <https://doi.org/10.1016/j.ijhydene.2022.01.064>.
- [8] Kasimalla VK, G NS, Velisala V. A review on energy allocation of fuel cell/battery/ultracapacitor for hybrid electric vehicles. *Int J Energy Res* 2018;42(14):4263–83. <https://doi.org/10.1002/er.4166>.
- [9] Guzzella L, Sciarretta A. *Vehicle propulsion systems*. Springer Berlin Heidelberg; 2013. <https://doi.org/10.1007/978-3-642-35913-2>.
- [10] Serrao L, Onori S, Rizzoni G. A comparative analysis of energy management strategies for hybrid electric vehicles. *J Dyn Syst Meas Control* Mar. 2011;133(3). <https://doi.org/10.1115/1.4003267>.
- [11] Ferrara A, Hametner C. Rule-based energy management strategy of fuel cell/ultracapacitor/battery vehicles: winner of the IEEE VTS motor vehicles challenge 2020. In: 2020 IEEE vehicle power and propulsion conference (VPPC). IEEE; 2020. <https://doi.org/10.1109/vppc49601.2020.9330930>.
- [12] Yue M, Jemei S, Gouriveau R, Zerhouni N. Review on health-conscious energy management strategies for fuel cell hybrid electric vehicles: degradation models and strategies. *Int J Hydrogen Energy* 2019;44(13):6844–61. <https://doi.org/10.1016/j.ijhydene.2019.01.190>.
- [13] Wang Y, Moura SJ, Advani SG, Prasad AK. Power management system for a fuel cell/battery hybrid vehicle incorporating fuel cell and battery degradation. *Int J Hydrogen Energy* 2019;44(16):8479–92. <https://doi.org/10.1016/j.ijhydene.2019.02.003>.
- [14] Fu Z, Zhu L, Tao F, Si P, Sun L. Optimization based energy management strategy for fuel cell/battery/ultracapacitor hybrid vehicle considering fuel economy and fuel cell lifespan. *Int J Hydrogen Energy* 2020;45(15):8875–86. <https://doi.org/10.1016/j.ijhydene.2020.01.017>.
- [15] Iqbal M, Ramadan HS, Becherif M. Health-aware frequency separation method for online energy management of fuel cell hybrid vehicle considering efficient urban utilization. *Int J Hydrogen Energy* 2021;46(29):16030–47. <https://doi.org/10.1016/j.ijhydene.2021.02.072>.
- [16] Luca R, Whiteley M, Neville T, Shearing PR, Brett DJ. Comparative study of energy management systems for a hybrid fuel cell electric vehicle - a novel mutative fuzzy logic controller to prolong fuel cell lifetime. *Int J Hydrogen Energy* 2022;47(57):24042–58. <https://doi.org/10.1016/j.ijhydene.2022.05.192>.
- [17] Ferrara A, Jakubek S, Hametner C. Energy management of heavy-duty fuel cell vehicles in real-world driving scenarios: robust design of strategies to maximize the hydrogen economy and system lifetime. *Energy Convers Manag* 2021;232:113795. <https://doi.org/10.1016/j.enconman.2020.113795>.
- [18] Ferrara A, Okoli M, Jakubek S, Hametner C. Energy management of heavy-duty fuel cell electric vehicles: model predictive control for fuel consumption and lifetime optimization. *IFAC-PapersOnLine* 2020;53(2):14205–10. <https://doi.org/10.1016/j.ifacol.2020.12.1053>.
- [19] Zendegan S, Ferrara A, Jakubek S, Hametner C. Predictive battery state of charge reference generation using basic route information for optimal energy management of heavy-duty fuel cell vehicles. *IEEE Trans Veh Technol* 2021;70(12):12517–28. <https://doi.org/10.1109/tvt.2021.3121129>.

- [20] Ambuhl D, Guzzella L. Predictive reference signal generator for hybrid electric vehicles. *IEEE Trans Veh Technol* 2009;58(9):4730–40. <https://doi.org/10.1109/tvt.2009.2027709>.
- [21] Du Y, Zhao Y, Wang Q, Zhang Y, Xia H. Trip-oriented stochastic optimal energy management strategy for plug-in hybrid electric bus. *Energy* 2016;115:1259–71. <https://doi.org/10.1016/j.energy.2016.09.056>.
- [22] Shen D, Lu L, Müller S. Utilization of predictive information to optimize driving and powertrain control of series hybrid vehicles. *Automotive and Engine Technology* 2017;2(1–4):39–47. <https://doi.org/10.1007/s41104-017-0016-6>.
- [23] Liu H, Yao Y, Wang J, Qin Y, Li T. A control architecture to coordinate energy management with trajectory tracking control for fuel cell/battery hybrid unmanned aerial vehicles. *Int J Hydrogen Energy* Mar 2022. <https://doi.org/10.1016/j.ijhydene.2022.03.036>.
- [24] Ahluwalia R, Wang X, Star A, Papadias D. Performance and cost of fuel cells for off-road heavy-duty vehicles. *Int J Hydrogen Energy* 2022;47(20):10990–1006. <https://doi.org/10.1016/j.ijhydene.2022.01.144>.
- [25] Fu Z, Chen Q, Zhang L, Zhang H, Deng Z. Research on ADHDP energy management strategy for fuel cell hybrid power system. *Int J Hydrogen Energy* 2021;46(57):29432–42. <https://doi.org/10.1016/j.ijhydene.2021.02.055>.
- [26] Yuan H-B, Zou W-J, Jung S, Kim Y-B. Optimized rule-based energy management for a polymer electrolyte membrane fuel cell/battery hybrid power system using a genetic algorithm. *Int J Hydrogen Energy* 2022;47(12):7932–48. <https://doi.org/10.1016/j.ijhydene.2021.12.121>.
- [27] Sun X, Zhou Y, Huang L, Lian J. A real-time PMP energy management strategy for fuel cell hybrid buses based on driving segment feature recognition. *Int J Hydrogen Energy* 2021;46(80):39983–40000. <https://doi.org/10.1016/j.ijhydene.2021.09.204>.
- [28] Wu P, Partridge J, Anderlini E, Liu Y, Bucknall R. Near-optimal energy management for plug-in hybrid fuel cell and battery propulsion using deep reinforcement learning. *Int J Hydrogen Energy* 2021;46(80):40022–40. <https://doi.org/10.1016/j.ijhydene.2021.09.196>.
- [29] Huo W, Chen D, Tian S, Li J, Zhao T, Liu B. Lifespan-consciousness and minimum-consumption coupled energy management strategy for fuel cell hybrid vehicles via deep reinforcement learning. *Int J Hydrogen Energy* 2022;47(57):24026–41. <https://doi.org/10.1016/j.ijhydene.2022.05.194>.
- [30] Venkatasatish R, Dhanamjayulu C. Reinforcement learning based energy management systems and hydrogen refuelling stations for fuel cell electric vehicles: an overview. *Int J Hydrogen Energy* 2022;47(64):27646–70. <https://doi.org/10.1016/j.ijhydene.2022.06.088>.
- [31] Gao H, Wang Z, Yin S, Lu J, Guo Z, Ma W. Adaptive real-time optimal energy management strategy based on equivalent factors optimization for hybrid fuel cell system. *Int J Hydrogen Energy* 2021;46(5):4329–38. <https://doi.org/10.1016/j.ijhydene.2020.10.205>.
- [32] Han X, Li F, Zhang T, Zhang T, Song K. Economic energy management strategy design and simulation for a dual-stack fuel cell electric vehicle. *Int J Hydrogen Energy* 2017;42(16):11584–95. <https://doi.org/10.1016/j.ijhydene.2017.01.085>.
- [33] Rudolf T, Schurmann T, Schwab S, Hohmann S. Toward holistic energy management strategies for fuel cell hybrid electric vehicles in heavy-duty applications. *Proc IEEE* 2021;109(6):1094–114. <https://doi.org/10.1109/jproc.2021.3055136>.
- [34] Xu L, Mueller CD, Li J, Ouyang M, Hu Z. Multi-objective component sizing based on optimal energy management strategy of fuel cell electric vehicles. *Appl Energy* 2015;157:664–74. <https://doi.org/10.1016/j.apenergy.2015.02.017>.
- [35] Jain M, Desai C, Williamson S. Genetic algorithm based optimal powertrain component sizing and control strategy design for a fuel cell hybrid electric bus. In: *IEEE vehicle power and propulsion conference*. IEEE; 2009. <https://doi.org/10.1109/vppc.2009.5289740>.
- [36] Tazelaar E, Shen Y, Veenhuizen P, Hofman T, van den Bosch P. Sizing stack and battery of a fuel cell hybrid distribution truck, *Oil & Gas Science and Technology. Revue d'IFP Energies nouvelles* 2012;67(4):563–73. <https://doi.org/10.2516/ogst/2012014>.
- [37] Hu X, Murgovski N, Johannesson LM, Egardt B. Optimal dimensioning and power management of a fuel cell/battery hybrid bus via convex programming. *IEEE ASME Trans Mechatron* 2015;20(1):457–68. <https://doi.org/10.1109/tmech.2014.2336264>.
- [38] Hu Z, Li J, Xu L, Song Z, Fang C, Ouyang M, Dou G, Kou G. Multi-objective energy management optimization and parameter sizing for proton exchange membrane hybrid fuel cell vehicles. *Energy Convers Manag* 2016;129:108–21. <https://doi.org/10.1016/j.enconman.2016.09.082>.
- [39] Wu X, Hu X, Yin X, Li L, Zeng Z, Pickert V. Convex programming energy management and components sizing of a plug-in fuel cell urban logistics vehicle. *J Power Sources* 2019;423:358–66. <https://doi.org/10.1016/j.jpowsour.2019.03.044>.
- [40] Fletcher T, Ebrahimi K. The effect of fuel cell and battery size on efficiency and cell lifetime for an l7e fuel cell hybrid vehicle. *Energies* 2020;13(22):5889. <https://doi.org/10.3390/en13225889>.
- [41] Feng Y, Dong Z. Integrated design and control optimization of fuel cell hybrid mining truck with minimized lifecycle cost. *Appl Energy* 2020;270:115164. <https://doi.org/10.1016/j.apenergy.2020.115164>.
- [42] Xun Q, Murgovski N, Liu Y. Joint component sizing and energy management for fuel cell hybrid electric trucks. *IEEE Trans Veh Technol* 2022;1. <https://doi.org/10.1109/tvt.2022.3154146>.
- [43] Gaikwad SD, Ghosh PC. Sizing of a fuel cell electric vehicle: a pinch analysis-based approach. *Int J Hydrogen Energy* 2020;45(15):8985–93. <https://doi.org/10.1016/j.ijhydene.2020.01.116>.
- [44] Wolff S, Seidenfus M, Brönnner M, Lienkamp M. Multi-disciplinary design optimization of life cycle eco-efficiency for heavy-duty vehicles using a genetic algorithm. *J Clean Prod* 2021;318:128505. <https://doi.org/10.1016/j.jclepro.2021.128505>.
- [45] Sim K, Vijayagopal R, Kim N, Rousseau A. Optimization of component sizing for a fuel cell-powered truck to minimize ownership cost. *Energies* 2019;12(6):1125. <https://doi.org/10.3390/en12061125>.
- [46] Capgemini. Fit for net-zero: 55 Tech Quests to accelerate Europe's recovery and pave the way to climate neutrality. October 2020. <https://www.capgemini.com/wp-content/uploads/2020/10/Net-zero-main-report-2020.pdf>.
- [47] Wilson A, Kleen G, Papageorgopoulos D. Fuel cell system cost 2017. November 2017, https://www.hydrogen.energy.gov/pdfs/17007_fuel_cell_system_cost_2017.pdf.
- [48] Goldie-Scot L. A behind the scenes take on lithium-ion battery prices. March 2019. <https://about.bnef.com/blog/behind-scenes-take-lithium-ion-battery-prices/>.
- [49] Haidl, Buchroithner Schweighofer, Bader Wegleiter. Lifetime analysis of energy storage systems for sustainable transportation. *Sustainability* 2019;11(23):6731. <https://doi.org/10.3390/su11236731>.
- [50] Hesse H, Schimpe M, Kucevic D, Jossen A. Lithium-ion battery storage for the grid—a review of stationary battery

- storage system design tailored for applications in modern power grids. *Energies* 2017;10(12):2107. <https://doi.org/10.3390/en10122107>.
- [51] Han X, Lu L, Zheng Y, Feng X, Li Z, Li J, Ouyang M. A review on the key issues of the lithium ion battery degradation among the whole life cycle. *eTransportation* 2019;1:100005. <https://doi.org/10.1016/j.etrans.2019.100005>.
- [52] Wang Y, Zhou Z, Botterud A, Zhang K, Ding Q. Stochastic coordinated operation of wind and battery energy storage system considering battery degradation. *Journal of Modern Power Systems and Clean Energy* 2016;4(4):581–92. <https://doi.org/10.1007/s40565-016-0238-z>.
- [53] Rechargeable batteries. In: *Batteries for portable devices*. Elsevier; 2005. p. 135. <https://doi.org/10.1016/b978-044451672-5/50005-3>.
- [54] Sundstrom O, Guzzella L. A generic dynamic programming matlab function. *IEEE International Conference on Control Applications, IEEE*; 2009. <https://doi.org/10.1109/cca.2009.5281131>.
- [55] McKay MD, Beckman RJ, Conover WJ. A comparison of three methods for selecting values of input variables in the analysis of output from a computer code. *Technometrics* 1979;21(2):239. <https://doi.org/10.2307/1268522>.
- [56] Ferrara A, Zendegan S, Koegeler H-M, Gopi S, Huber M, Pell J, Hametner C. Optimal calibration of an adaptive and predictive energy management strategy for fuel cell electric trucks. *Energies* 2022;15(7):2394. <https://doi.org/10.3390/en15072394>.
- [57] Pei P, Chang Q, Tang T. A quick evaluating method for automotive fuel cell lifetime. *Int J Hydrogen Energy* 2008;33(14):3829–36. <https://doi.org/10.1016/j.ijhydene.2008.04.048>.
- [58] Ferrara A, Hametner C. Impact of energy management strategies on hydrogen consumption and start-up/shut-down cycles in fuel cell-ultracapacitor-battery vehicles. *IEEE Trans Veh Technol* 2021;1. <https://doi.org/10.1109/tvt.2021.3127582>.
- [59] Fletcher T, Thring R, Watkinson M. An energy management strategy to concurrently optimise fuel consumption & PEM fuel cell lifetime in a hybrid vehicle. *Int J Hydrogen Energy* 2016;41(46):21503–15. <https://doi.org/10.1016/j.ijhydene.2016.08.157>.
- [60] Zhang C, Zhang Y, Huang Z, Lv C, Hao D, Liang C, Deng C, Chen J. Real-time optimization of energy management strategy for fuel cell vehicles using inflated 3d inception long short-term memory network-based speed prediction. *IEEE Trans Veh Technol* 2021;70(2):1190–9. <https://doi.org/10.1109/tvt.2021.3051201>.
- [61] Deng K, Liu Y, Hai D, Peng H, Löwenstein L, Pischinger S, Hameyer K. Deep reinforcement learning based energy management strategy of fuel cell hybrid railway vehicles considering fuel cell aging. *Energy Convers Manag* 2022;251:115030. <https://doi.org/10.1016/j.enconman.2021.115030>.